

Electrochemical Pumping for Challenging Hydrogen Separations

Gokul Venugopalan, Deepra Bhattacharya, Evan Andrews, Luis Briceno-Mena, José Romagnoli, John Flake, and Christopher G. Arges*



Cite This: *ACS Energy Lett.* 2022, 7, 1322–1329



Read Online

ACCESS |



Metrics & More

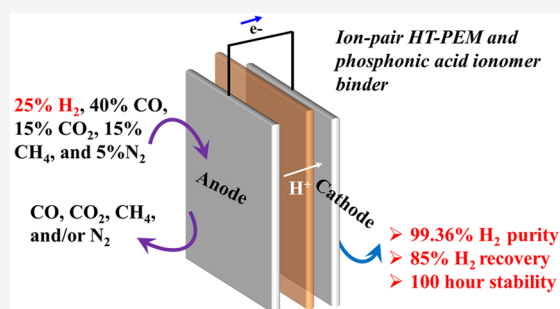


Article Recommendations



Supporting Information

ABSTRACT: Conventional hydrogen separations from reformed hydrocarbons often deploy a water gas shift (WGS) reactor to convert CO to CO₂, followed by adsorption processes to achieve pure hydrogen. The purified hydrogen is then fed to a compressor to deliver hydrogen at high pressures. Electrochemical hydrogen pumps (EHPs) featuring proton-selective polymer electrolyte membranes (PEMs) represent an alternative separation platform with fewer unit operations because they can simultaneously separate and compress hydrogen continuously. In this work, a high-temperature PEM (HT-PEM) EHP purified hydrogen to 99.3%, with greater than 85% hydrogen recovery for feed mixtures containing 25–40% CO. The ion-pair HT-PEM and phosphonic acid ionomer binder enabled the EHP to be operated in the temperature range from 160 to 220 °C. The ability to operate the EHP at an elevated temperature allowed the EHP to purify hydrogen from gas feeds with large CO contents at 1 A cm⁻². Finally, the EHP with the said materials displayed a small performance loss of 12 μV h⁻¹ for purifying hydrogen from syngas for 100 h at 200 °C.



Natural gas prices over the past 15 years have experienced a precipitous drop due to innovations made in fracking technology and the extraction of this resource from shale layers.¹ The 32% reduction in CO₂ emissions from the electric power sector in the United States since 2005 is largely attributed to natural gas supplanting coal for burning in thermal electric plants, as it is cheaper and a cleaner fuel.² However, natural gas combustion still yields CO₂, a greenhouse gas (GHG) and a large contributor to climate disruption. Meeting the ambitious goal of a 50% reduction in GHG emissions by 2030, as outlined by the Biden Administration,³ or the 2016 Paris Agreement⁴ to limit global temperature increases below 2 °C requires the continued adoption of renewable energy sources, such as solar, nuclear, and wind; the proliferation of energy storage technologies, such as batteries; and the implementation of blue, green, and pink hydrogen as energy vectors and chemical feedstocks in the global economy. As renewables displace natural gas as an energy source, there is still significant value in harnessing natural gas as a source of carbon and hydrogen for chemical manufacturing (e.g., surfactants and plastics) and the production of fuels.⁵

Over 90% of hydrogen used in the United States is derived from steam methane reforming (SMR).⁶ The SMR process uses natural gas as a feedstock and generates syngas, a mixture that primarily consists of hydrogen, carbon monoxide (CO),

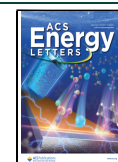
and some carbon dioxide (CO₂). It is important to note that numerous chemical processes⁷ use hydrogen from SMR, e.g., ammonia production for fertilizers by the Haber–Bosch process, desulfurization in petrochemical processes, metal refining, chemical hydrogenation, and semiconductor manufacturing. The hydrogen used in these processes often requires separation from syngas.

Conventional hydrogen separations encompass several different methods⁸ such as cryogenic cooling,⁹ thermal metal hydride adsorption,¹⁰ pressure swing adsorption,¹¹ and palladium membranes.¹² Electrochemical hydrogen pumps (EHPs)¹³ featuring proton-selective polymer electrolyte membranes (PEMs) represent an alternative separation platform that can simultaneously separate and compress hydrogen continuously. Adsorption processes do not operate continuously because they saturate and require regeneration. Palladium membranes require temperatures over 350 °C for hydrogen separation, and they cannot be used for compression.

Received: January 4, 2022

Accepted: March 4, 2022

Published: March 11, 2022



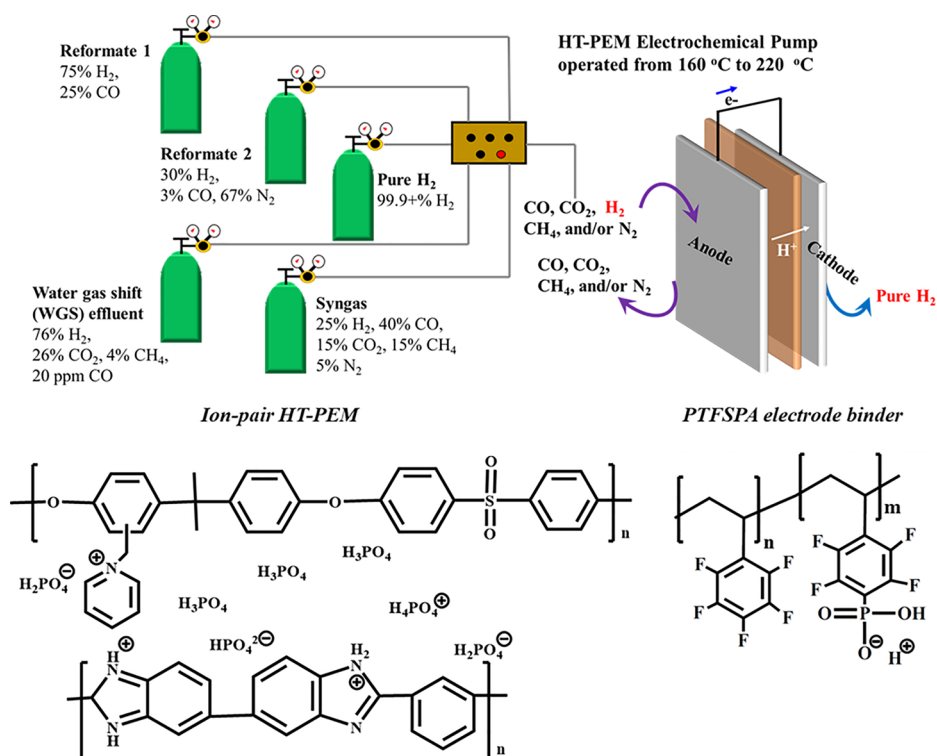


Figure 1. (a) HT-PEM EHP experimental setup that can purify hydrogen from several types of hydrogen mixtures containing CO, CO₂, CH₄, and N₂. (b) The chemical structures of the ion-pair HT-PEM and electrode ionomer binder. PTFSPA = poly(tetrafluorostyrene phosphonic acid-co-pentafluorostyrene), a random copolymer.

EHPs were originally developed by General Electric¹⁴ with the emergence of perfluorosulfonic acid (PFSA) membranes, such as Nafion, and have been used for hydrogen compression and reuse in various industrial settings.¹³ PFSA membranes do not function over 100 °C because they need condensed water within the membrane to mediate proton conduction.¹⁵ Platinum electrocatalysts are the choice materials for the hydrogen oxidation reaction (HOR) and the hydrogen evolution reaction (HER) in EHPs that operate under acidic conditions. Reformed natural gas and other fossil fuels, however, contain CO that strongly adsorbs to platinum at low temperatures, making low-temperature PEM EHPs ineffective for hydrogen separations of gas mixtures containing CO. Concentrations of CO at 100 ppm or less are known to incur significant overpotentials that hamper the performance of EHPs.^{16,34}

High-temperature polymer electrolyte membranes (HT-PEMs) based on phosphoric acid (H₃PO₄) imbedded polybenzimidazole (PBI) enable EHP operation at elevated temperatures (e.g., 180 °C) for hydrogen separations of mixtures containing CO.^{17,18} However, there have been limited demonstrations of EHPs using PBI–H₃PO₄ separators for hydrogen separations. To date, these HT-PEM EHP studies have only processed hydrogen up to 3% CO at 1.6% RH and 160–200 °C. Operating the EHP at high temperatures (200–250 °C) significantly improves the Pt catalyst's tolerance to CO and other impurities in the inlet gas stream, eventuating in the better utilization of the Pt catalyst for carrying out the hydrogen separation. Commercial PBI from Fumatech is unstable at temperatures above 180 °C for extended periods of time because H₃PO₄ evaporates from PBI.^{19,20} Additionally, PBI membranes have low stabilities under high inlet

stoichiometric flow rates, hence reducing the tolerance to higher CO concentrations in the inlet anode feed.

Ion-pair HT-PEMs based on H₃PO₄-imbibed polycations (or polycation–PBI blends) have shown superior performance compared to PBI–H₃PO₄ as they are stable in the presence of water vapor (e.g., 40% RH at 80 °C) and at temperatures high as 240 °C while also providing excellent proton conductivities (≥ 0.25 S cm⁻¹, ASR ≤ 15 mΩ cm²).^{15,20} The remarkable performance of the ion-pair HT-PEMs is attributed to cation moieties in the polymer host that anchor phosphate anions, mitigate the loss of H₃PO₄ from the polymer under challenging conditions, and spur greater hydrogen bonding frustration of the imbibed H₃PO₄, which fosters proton conduction. Pairing the ion-pair HT-PEMs with electrodes that featured poly(tetrafluorostyrene phosphonic acid-co-pentafluorostyrene) (PTFSPA) ionomer binders resulted in remarkable fuel cell performance,²¹ e.g., a power density up to 1.7 W cm⁻². Mixing the PTFSPA with Nafion as the electrode binder resulted in a fuel cell peak power density of 2 W cm⁻² at 200 °C with hydrogen and oxygen.²²

In our previous work,²³ we showcased the advancement of hydrogen reaction kinetics and gas permeability using phosphonic acid-functionalized polymer electrolytes, PTFSPA, compared to conventional those of H₃PO₄-doped polycation electrolytes using a nanostructured electrocatalyst. The use of phosphonic acid ionomer binders over H₃PO₄-doped polycation electrolytes not only facilitated a better fuel cell power density²¹ but also showed a EHP with a very low polarization (1 A cm⁻² at 55 mV)²³ when pure hydrogen was used. The PTFSPA binders enable better performance because they promote hydrogen gas permeability and contain less phosphate-type anions, which are known to interfere with the platinum electrocatalyst.

This work demonstrates an EHP for purifying hydrogen to $\geq 99.3\%$ from reformed hydrocarbon mixtures (e.g., gases that contain 3%, 25%, and 40% CO) and water gas shift (WGS) reactor effluent mixtures (20 ppm CO). The EHP used an ion-pair HT-PEM and PTFSPA electrode binders. The polarization behaviors of the HT-EHPs were tested at high temperatures from 160 to 220 °C with 0% RH. The work is motivated by the fact that 90% of hydrogen today is attained from steam reforming methane found in natural gas, leading to a sizable CO concentration (often over 20 mol %). With the advent of ion-pair HT-PEMs and PTFSPA ionomer electrode binders that are thermally stable at temperatures up to 250 °C, it was posited that a HT-PEM EHP could be operated at temperatures greater than 200 °C for the first time by curtailing CO adsorption on the platinum electrocatalyst, which hinders the performance of the EHP. At 220 °C, the impact of CO on EHP cell polarization was minimized and the polarization of the EHP cell was governed by the hydrogen concentration in the anode feed. Furthermore, the hydrogen purity (HP), hydrogen recovery rate (HRR), power consumption, and power efficiency of syngas mixtures and WGS effluents were tested. The EHP featuring the ion-pair HT-PEM and PTFSPA electrode binders had a HP greater than 99.3%, with a HRR greater than 93% in separating syngas and WGS effluents at 200 °C. The ion-pair HT-PEM and PTFSPA electrode binders were stable for 100 h at 200 °C for purifying hydrogen from syngas at 0.25 A cm⁻², with a cell voltage loss of 12 μ V h⁻¹.

Figure 1a depicts the experimental setup of several gas mixtures containing hydrogen plumbed to a single-cell HT-PEM EHP unit. The four gas mixtures were (i) syngas (25% H₂, 40% CO, 15% CO₂, 15% CH₄, and 5% N₂), (ii) reformat 1 (75% H₂ and 25% CO), (iii) reformat 2 (30% H₂ and 3% CO with a N₂ balance), and (iv) a WGS effluent (76% H₂, 20% CO₂, 5% CH₄, and 20 ppm CO). The EHP's performance with the various gas mixtures was benchmarked against pure hydrogen data from our previous work.²³ Model reformat mixture compositions, namely, reformat 1 and reformat 2, were selected based on literature precedent.^{18,24} These mixtures represent compositions from reformed methanol or other hydrocarbons. The syngas mixture used in this work is a challenging mixture for hydrogen separations via an EHP because of the large CO content (in this case 40%). However, most of the global hydrogen demand is satisfied from SMR and thus the separation platform for purifying hydrogen needs to tolerate sizable CO concentrations. To deal with the CO, a WGS reactor is often employed to oxidize the CO to CO₂, a species that interferes less with platinum electrocatalysts and is less toxic. In this work, we show that the HT-PEM EHP can purify hydrogen from each of these gas mixtures to $>99.3\%$ and with a HRR over 93%. Adopting materials that enable higher temperature operation (e.g., 200–220 °C) substantially reduces the polarization for separation and enables higher current density operation (i.e., a greater flux of purified hydrogen).

The chemical structures of the ion-pair HT-PEM and the ionomer electrode binder used in the EHP are shown in Figure 1b. The HT-PEM is quaternary benzylpyridinium poly(arylene ether sulfone) blended with PBI imbided with H₃PO₄ (QPPSf-PBI H₃PO₄). In our previous work,²⁰ ion-pair HT-PEM displayed a high proton conductivity (>250 mS cm⁻¹) and stability at 220 °C. The PTFSPA binder does not contain any liquid acid and demonstrates a proton conductivity of 2 mS cm⁻¹ without activation.²³ Activating PTFSPA with a small

amount of H₃PO₄ enhances its conductivity to 60 mS cm⁻¹. The gas diffusion electrodes (GDEs) used in the EHP feature platinum nanoparticles decorated on high-surface-area graphitic carbon with a PTFSPA binder. The platinum loading in the anode and cathode was 1 mg_{Pt} cm⁻². This platinum loading is identical to other HT-PEM EHP reports that used BASF electrodes.^{17,18}

Figure S1a–e corresponds to the steady-state EHP polarization curves with different hydrogen gas mixtures (or pure hydrogen) at 160, 180, 200, and 220 °C. In each of these panels, the polarization was reduced when the cell temperature moved from 160 to 220 °C. The reduction in polarization was more prominent for the gas mixtures that contained 25–40% CO (e.g., reformat 1 and syngas). For the syngas feed that contained 40% CO, the EHP with the ion-pair HT-PEM and GDEs with PTFSPA binders operated at 1 A cm⁻² and 0.4 V when the cell temperature was 220 °C. Temperature had a large impact on EHP performance, especially with syngas feeds. The cell voltage was reduced by 0.97 V when the cell temperature moved from 160 to 220 °C when the cell was fixed at 0.3 A cm⁻². The same increase in cell temperature for purifying hydrogen from reformat 1 at 0.5 A cm⁻² resulted in a cell voltage drop of 0.2 V. The reduction in polarization for syngas at temperatures greater than 200 °C could be attributed to (i) the higher proton conductivity of the PTFSPA and HT-PEM materials, (ii) greater hydrogen diffusivity across the PTFSPA electrode ionomer binder that covers the electrocatalyst, and (iii) the reduced CO adsorption on Pt leading to improved HOR and HER kinetics.

The concentration of hydrogen in the gas mixture fed to the anode also had a profound impact on polarization. Panels a and b in Figure 2 compare the polarization curves for the various gas mixtures at 220 and 200 °C, respectively. Interestingly, the syngas and reformat 2 curves in Figure 2a almost overlap at 220 °C despite the syngas having 13× more CO (40% versus 3% in reformat 2). Similarly, the traces in Figure 2a for reformat 1 and the WGS effluent also practically overlapped even though reformat 1 had significantly more CO (25% versus 0.02%, respectively). It is important to note that the hydrogen concentrations of syngas and reformat 2 range from 25% to 30% and their polarization curves are close to each other. Similarly, the hydrogen concentrations for reformat 1 and the WGS effluent range from 75% to 76% and their polarization curves are about the same. Figure 2a conveys that the polarization behavior is a stronger function of the hydrogen content in the gas mixture and that CO has a small impact on polarization. For the data sets at the next-lowest temperature (i.e., 200 °C), there is greater separation between syngas and reformat 2 and between the WGS effluent and reformat 1 because there is more CO in syngas than reformat 2 and more CO in reformat 1 than the WGS effluent. The salient observations from Figure 2a and b signal the following: (i) operating the HT-PEM EHP at 220 °C minimizes the impact CO has on the EHP's performance and (ii) the polarization of the EHP is a strong function of the hydrogen content in the mixture. With respect to point ii, Nguyen²⁵ observed a relationship between low-temperature PEM EHP polarization and the hydrogen content in the anode feed (balanced by argon gas). The greater EHP polarization with a lower hydrogen content in the anode is attributed to increase in the Nernstian potential in addition to larger concentration overpotential and activation overpotential values. Furthermore, the lower partial pressure of hydrogen

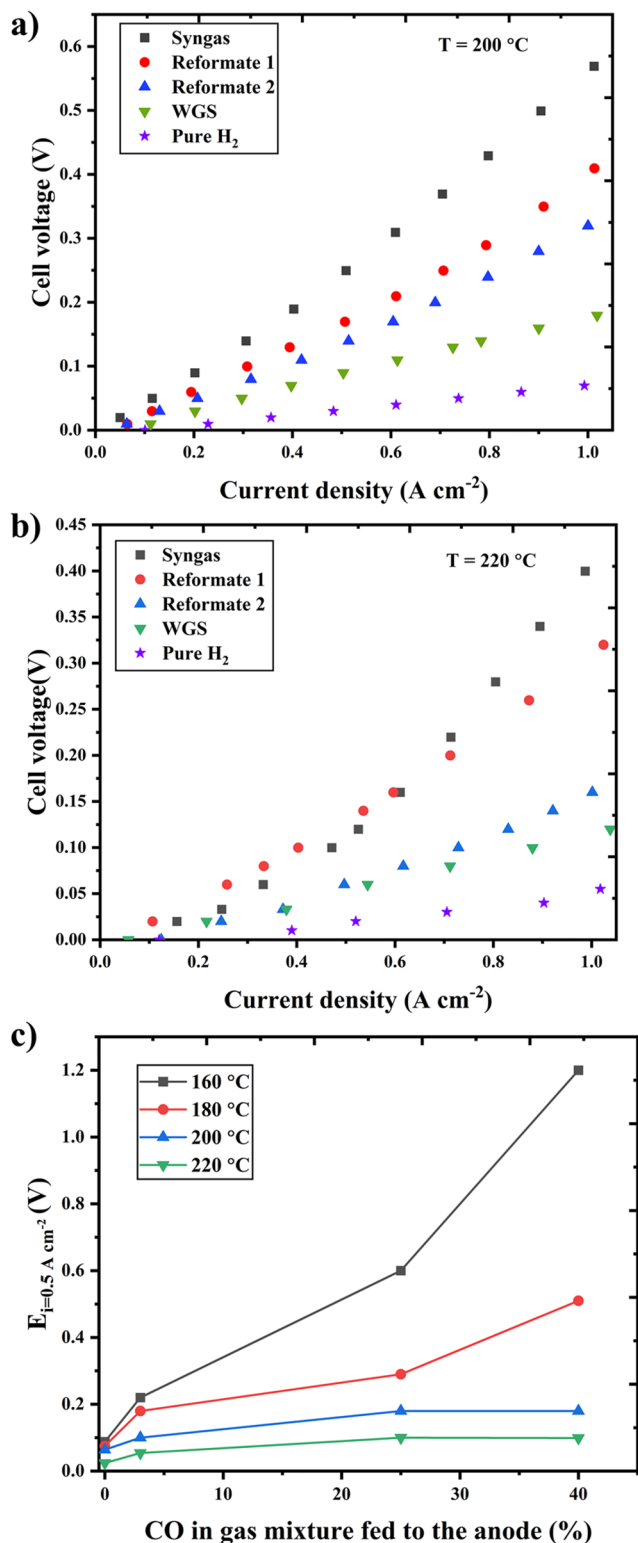


Figure 2. EHP polarization curves for the different gas mixtures and pure H₂ at (a) 200 and (b) 220 °C. The traces in panel a demonstrate that the polarization is governed by the H₂ concentration in the anode, as syngas and reformat 2 contain 25% to 30% H₂ respectively, and WGS effluent, and reformat 1 contain 75–76% H₂. At 200 °C, a slightly lower temperature, the polarization behavior is also a function of the H₂ content in the gas feed, but gas streams for almost the same H₂ contents show greater polarization if they contain more CO. (c) Cell voltage at 0.5 A cm⁻² vs the CO content in the H₂ gas mixture. The gas mixture

Figure 2. continued

with 40% CO is syngas. The gas mixture with 25% CO is reformat 1. The gas mixture with 3% CO is reformat 2. The gas mixture with 20 ppm is the WGS effluent. At 220 °C, the cell polarization behavior is only affected by 90 mV or less when the CO content is varied from 40% to 0%. Conversely, there is an over 1 V difference between the 40% and 0% CO concentrations at 160 °C.

in the anode causes greater mass transfer resistance and leads to a lower hydrogen permeability across the ionomer binder. The exchange current density is a function of the concentration of the reactant at the electrocatalyst surface; thus, a lower hydrogen content in the bulk will lower the exchange current density and increase the activation overpotential.

To reinforce the observations from Figure 2a and b, Figure 2c plots the cell voltage at 0.5 A cm⁻² versus the CO concentration in the mixture for different cell temperatures. Driving the cell temperature from 160 to 220 °C flattens the cell voltage values across the different CO concentration values. Increasing the cell temperature reduces the propensity of CO to adsorb on the PGM surface in the anode and block catalyst sites for the HOR. Panels a–c in Figure 2 convey that increasing the cell temperature from 160 to 220 °C minimized the impact CO had on the EHP polarization.

Table 1 demonstrates that over 99.3% hydrogen gas was generated at the cathode for each gas mixture. For the challenging syngas separation, only 0.3% CO showed up in the cathode effluent despite 40% CO being present in the anode gas stream. The composition of the cathode effluent was examined at two different steady-state current density values (0.25 and 1 A cm⁻²). The current density had a negligible effect on the cathode composition. Overall, the HT-PEM was a good barrier to contaminants and fostered over 99% purity at the cathode. Table 2 presents the hydrogen recovery rate (HRR), power efficiency, and power consumption from HT-PEM EHP experiments with different hydrogen gas mixtures at 200 °C and at two different steady-state current density values (0.25 A and 1 A cm⁻²). These data were analyzed at T = 200 °C for comparison against other EHP data in the literature.^{17,18} The large power efficiency (%) of the HT-PEM EHP is attributed to the reduction in CO adsorption and the improved HOR and HER kinetics at 200 °C. The HRR, power efficiency, and power consumption were calculated using eqs S1–S3. Most literature data for HRR and HP are for purifying hydrogen from WGS effluents and the use of pressure swing adsorption (PSA) and EHP units. Figure S2 compares the HRR and HP data from this work against other peer-reviewed data from the literature.^{17,26–34} The ion-pair HT-PEM EHP in this work represents the largest HRR value to date (98.84%). It is important to note that the data analyses were performed at 200 °C because the QPPSf-PBI H₃PO₄ ion-pair HT-PEM experiences a mechanical failure under compression at 220 °C within 30 h,²⁰ and other data in the literature for benchmarking are only available at 200 °C. The ion-pair HT-PEM was previously shown to be stable in the temperature range for 180 to 200 °C for over 80 h in a fuel cell device.²⁰ Figure S3 compares the EHP polarization data attained from this work against literature data obtained using a PBI-type separator when hydrogen was purified from reformat 2 and a WGS reactor effluent. These gas streams contain 3% CO and 20 ppm of CO, respectively. The EHP with the ion-pair HT-

Table 1. Cathode Effluent Gas Composition at 200 °C from EHP Experiments

gas mixtures	syngas		reformat 1		WGS		reformat 2	
current density ($A\text{ cm}^{-2}$)	0.25	1	0.25	1	0.25	1	0.25	1
cathode outlet composition								
H ₂ (%)	99.36	99.65	99.75	99.84	99.40	99.80	99.78	99.85
CO (%)	0.300	0.205	0.25	0.16	0.0002	0.0025	0.006	0.003
CO ₂ (%)	0.288	0.145			0.339	0.199		
N ₂ (%)	0.007	0.005			0.008	0.003	0.378	0.108
CH ₄ (%)	0.051	0.032			0.09	0.07		

Table 2. Hydrogen Recovery Rate (HRR), Power Efficiency, and Power Consumption for Purifying Hydrogen from Various Gas Mixtures Using the HT-PEM EHP at $T = 200\text{ }^{\circ}\text{C}$

gas mixtures	syngas		reformat 1		WGS		reformat 2	
current density ($A\text{ cm}^{-2}$)	0.25	1	0.25	1	0.25	1	0.25	1
hydrogen recovery rate (%)	85.49	93.80	89.66	95.43	93.74	98.84	93.16	96.73
power efficiency (%)	85.63	95.14	89.82	96.41	93.81	99.13	93.24	97.33
power consumption (mW cm^{-2})	15.5	543	17.4	387	6.73	115	9.16	237

PEM and GDEs with PTFSPA binders matched the polarization with state-of-the-art data with a WGS reactor effluent.

Because there are no other HT-PEM EHP studies with ion-pair HT-PEM separators for purifying hydrogen from gas mixtures containing CO amounts over 3%, Figure S4a and b compares the HT-PEM EHP polarization data from this work with syngas against polarization data with a Celazole PBI HT-PEM separators at 200 °C. Fumatech PBI separators are no longer commercially available. The Celazole PBI separator was prepared from a dispersion that was attained from PBI Performance Products. Compared to the ion-pair HT-PEM, greater cell polarization was observed with the PBI HT-PEM, highlighting the superiority of the ion-pair HT-PEM for EHPs. At 0.5 $A\text{ cm}^{-2}$ and 220 °C, the cell voltage with the ion-pair HT-PEM was 600 mV lower when compared to that of the PBI HT-PEM. The electrodes were identical for these experiments. The greater polarization with the PBI separator was attributed to its higher area specific resistance (ASR) compared to that of the ion-pair HT-PEM (0.23 $\Omega\text{ cm}^2$ versus 0.02 $\Omega\text{ cm}^2$).

Figure 3a reports the change in cell voltage at 200 °C over 100 h with a steady-state current hold of 0.25 $A\text{ cm}^{-2}$ and syngas feed to the anode. The HT-PEM EHP with an ion-pair HT-PEM and PTFSA electrode binders only displayed an increase of 12 $\mu\text{V h}^{-1}$. During the stability test, simultaneous compression and separation for hydrogen was attempted. The cathode back pressure was 207 kPa higher than that of the anode. However, the low gas flow rate on the cathode made it difficult to sustain a differential pressure and thus the back pressure was lost at the 42 h time point. Future work will focus on modifying the hardware and setup for simultaneous separation and compression without the addition of a carrier gas at the cathode, which would dilute the hydrogen. Figure S4c compares the HT-PEM EHP stability using an ion-pair HT-PEM separator and PBI HT-PEM separator at 200 °C. The MEA with the PBI HT-PEM initially had a 3 \times higher cell voltage at 0.25 $A\text{ cm}^{-2}$, and the cell voltage increased by 3 mV h^{-1} over 24 h. The EHP with the ion-pair HT-PEM separator was more stable than the EHP with the Celazole PBI HT-PEM separator.

The purity of the hydrogen emanating from the cathode during the 100 h stability test with the ion-pair HT-PEM was monitored at the 40 h time point and the 100 h time point.

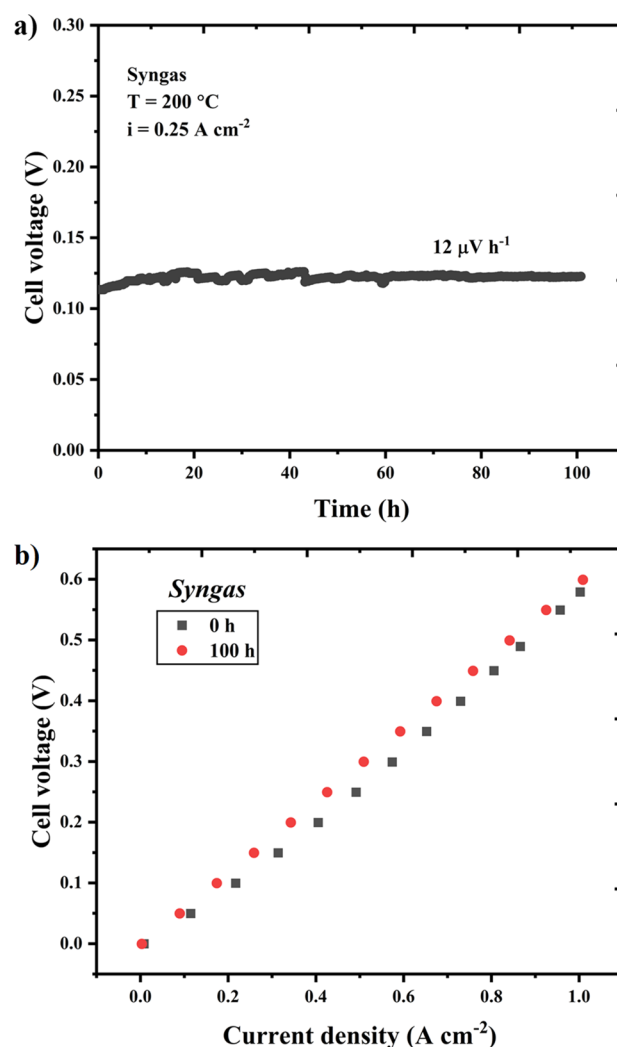


Figure 3. (a) HT-PEM EHP stability test at 200 °C and a constant current of 0.25 $A\text{ cm}^{-2}$ with a syngas feed to the anode. (b) HT-PEM EHP polarization at 200 °C with syngas before and after the 100 h stability test.

The purity values were 99.5% and 99.4% hydrogen, respectively, and the CO content in the cathode was under

0.27%. Table S1 provides the gas composition values collected at the different time points during the stability test. Figure 3b compares the polarization curves obtained before the stability test and those obtained after the 100 h stability test. There is some performance loss after the stability test, but the average current density difference for a given cell voltage value is 0.045 A cm⁻², a relatively small value given that up to 1 A cm⁻² can be extracted from the cell.

In summary, Figure 3a and b demonstrates that the EHP featuring the ion-pair HT-PEM and PTFSPA electrode binders is stable at 200 °C for 100 h, with a minimal performance loss of 12 μV h⁻¹ for purifying hydrogen from syngas. Additional investigations will be performed in future work to understand HOR and HER kinetics and the hydrogen diffusivity as a function of temperature in porous electrodes with various binder loadings using systematically controlled dilute hydrogen gas mixtures balanced with nitrogen. Other practical investigations will include engineering the membrane electrode assemblies to achieve higher current density values, greater hydrogen purity, and large differential pressures.

An EHP with an ion-pair HT-PEM separator and PTFSA binders in the gas diffusion electrodes purified hydrogen to 99.3% purity from syngas (25% H₂ and 40% CO) at 1 A cm⁻² with a cell voltage of 400 mV. The high current density operation of the EHP with the challenging gas feed was made possible by operating the EHP at 220 °C. This is the first demonstration showing that electrochemical pumping can be used to purify hydrogen from gas mixtures containing large CO concentrations at intermediate temperatures and high current density values. The only other report³⁵ on an EHP for purifying hydrogen from syngas (64% H₂, 32% CO, and 4% N₂) required an operation temperature of 800 °C because it used an inorganic solid electrolyte that had poor conductivity. Additionally, the HRR for purifying hydrogen to 99.3% purity from syngas was 85%, making the EHP a competitive platform for hydrogen separations from gas mixtures containing large CO concentrations. Finally, the HT-PEM was stable at 100 h for purifying syngas at 200 °C and only experienced a minor loss in performance (e.g., a 12 μV h⁻¹ increase under constant current operation). The ability of the HT-PEM EHP to carry out challenging hydrogen separations with syngas and reformates opens future opportunities to convert methane in natural gas to pure hydrogen without using a WGS reactor for various downstream processes, such as powering fuel cells, manufacturing chemicals, and refining metals. Additionally, the HT-PEM EHP demonstrated here can be useful for purifying hydrogen from gasified biomass.

■ ASSOCIATED CONTENT

SI Supporting Information

The Supporting Information is available free of charge at <https://pubs.acs.org/doi/10.1021/acseenergylett.1c02853>.

Experimental materials and methods; steady-state polarization curves; HP vs HRR for the HT-PEM EHP, normal-temperature PSA, elevated-temperature PSA, and sorption-enhanced WGS technologies; HT-PEM EHP performance comparison for an ion-pair HT-PEM and a PBI separator; HT-PEM EHP stability test comparison for the ion-pair HT-PEM and a PBI; and cathode effluent gas composition measure during the 100 h stability test (PDF)

■ AUTHOR INFORMATION

Corresponding Author

Christopher G. Arges – Department of Chemical Engineering, The Pennsylvania State University, University Park, Pennsylvania 16802, United States; orcid.org/0000-0003-1703-8323; Email: chris.arges@psu.edu

Authors

Gokul Venugopalan – Cain Department of Chemical Engineering, Louisiana State University, Baton Rouge, Louisiana 70803, United States; Chemistry and Nanoscience Research Center, National Renewable Energy Laboratory, Golden, Colorado 80401, United States; orcid.org/0000-0002-7332-4300

Deepra Bhattacharya – Department of Chemical Engineering, The Pennsylvania State University, University Park, Pennsylvania 16802, United States

Evan Andrews – Cain Department of Chemical Engineering, Louisiana State University, Baton Rouge, Louisiana 70803, United States

Luis Briceno-Mena – Cain Department of Chemical Engineering, Louisiana State University, Baton Rouge, Louisiana 70803, United States; orcid.org/0000-0003-3684-4232

José Romagnoli – Cain Department of Chemical Engineering, Louisiana State University, Baton Rouge, Louisiana 70803, United States; orcid.org/0000-0003-3682-1305

John Flake – Cain Department of Chemical Engineering, Louisiana State University, Baton Rouge, Louisiana 70803, United States; orcid.org/0000-0002-9187-3143

Complete contact information is available at:

<https://pubs.acs.org/10.1021/acseenergylett.1c02853>

Author Contributions

G.V. synthesized materials, fabricated HT-PEMs and GDEs, and performed all experiments with EHPs. D.B. performed all the baseline HT-PEM EHP performance measurements. E.A. measured the purity of the cathode gas streams and calibrated the gas chromatogram. G.V. and C.G.A. wrote the manuscript. All authors contributed to data analysis and the editing of the manuscript.

Notes

The authors declare the following competing financial interest(s): C.G.A. is a co-founder and owner of a startup company, Ionomer Solutions LLC, that is commercializing HT-PEM materials (US Patent Application 62/656,538) and HT-PEM EHP technology (US Patent Application 63/192,607) developed at Louisiana State University.

■ ACKNOWLEDGMENTS

This material is based on work supported by the U.S. Department of Energy's Office of Energy Efficiency and Renewable Energy (EERE) under the Advanced Manufacturing Office (AMO) Award no. DE-EE0009101. The views expressed herein do not necessarily represent the views of the U.S. Department of Energy or the United States Government. L.A.B. is thankful for the support received from Universidad de Costa Rica.

■ REFERENCES

(1) Peplow, M. How fracking is upending the chemical industry. *Nature* **2017**, *550* (7674), 26–28. Deutch, J. The Revolution in

Natural Gas. *Perspectives on Complex Global Challenges: Education, Energy, Healthcare, Security and Resilience* **2016**, 81–83.

(2) McGrath, G. Electric power sector CO₂ emissions drop as generation mix shifts from coal to natural gas. *U.S. Energy Information Administration*, 2021. <https://www.eia.gov/todayinenergy/detail.php?id=48296> (accessed 2021-09-16).

(3) FACT SHEET: President Biden Sets 2030 Greenhouse Gas Pollution Reduction Target Aimed at Creating Good-Paying Union Jobs and Securing U.S. Leadership on Clean Energy Technologies. *The White House*, 2021. <https://www.whitehouse.gov/briefing-room/statements-releases/2021/04/22/fact-sheet-president-biden-sets-2030-greenhouse-gas-pollution-reduction-target-aimed-at-creating-good-paying-union-jobs-and-securing-u-s-leadership-on-clean-energy-technologies/> (accessed 2021-09-16).

(4) FACT SHEET: President Biden Sets 2030 Greenhouse Gas Pollution Reduction Target Aimed at Creating Good-Paying Union Jobs and Securing U.S. Leadership on Clean Energy Technologies. *The White House*, 2021. <https://www.whitehouse.gov/briefing-room/statements-releases/2021/04/22/fact-sheet-president-biden-sets-2030-greenhouse-gas-pollution-reduction-target-aimed-at-creating-good-paying-union-jobs-and-securing-u-s-leadership-on-clean-energy-technologies/> (accessed 2021-09-16).

(5) Cullen, D. A.; Neyelin, K. C.; Ahluwalia, R. K.; Mukundan, R.; More, K. L.; Borup, R. L.; Weber, A. Z.; Myers, D. J.; Kusoglu, A. New roads and challenges for fuel cells in heavy-duty transportation. *Nature Energy* **2021**, *6*, 462–474.

(6) Hydrogen Production: Natural Gas Reforming. *energy.gov*. <https://www.energy.gov/eere/fuelcells/hydrogen-production-natural-gas-reforming> (accessed 2021-09-16).

(7) Ramachandran, R.; Menon, R. K. An overview of industrial uses of hydrogen. *Int. J. Hydrogen Energy* **1998**, *23* (7), 593–598.

(8) Du, Z.; Liu, C.; Zhai, J.; Guo, X.; Xiong, Y.; Su, W.; He, G. A Review of Hydrogen Purification Technologies for Fuel Cell Vehicles. *Catalysts* **2021**, *11* (3), 393.

(9) Aasadnia, M.; Mehrpooya, M.; Ghorbani, B. A novel integrated structure for hydrogen purification using the cryogenic method. *Journal of Cleaner Production* **2021**, *278*, 123872.

(10) Dunikov, D.; Blinov, D. Extraction of hydrogen from a lean mixture with methane by metal hydride. *Int. J. Hydrogen Energy* **2020**, *45* (16), 9914–9926.

(11) Sircar, S.; Golden, T. C. Purification of Hydrogen by Pressure Swing Adsorption. *Sep. Sci. Technol.* **2000**, *35* (5), 667–687.

(12) Rahimpour, M. R.; Samimi, F.; Babapoor, A.; Tohidian, T.; Mohebi, S. Palladium membranes applications in reaction systems for hydrogen separation and purification: A review. *Chemical Engineering and Processing: Process Intensification* **2017**, *121*, 24–49.

(13) Fishel, K.; Qian, G.; Eisman, G.; Benicewicz, B. C. Electrochemical Hydrogen Pumping. In *High Temperature Polymer Electrolyte Membrane Fuel Cells*; Li, Q., Ed.; Springer International Publishing, 2016; pp 527–540.

(14) Maget, H. J. R. Process for gas purification. US 3489670 A, 1964.

(15) Lee, K.-S.; Spendelow, J. S.; Choe, Y.-K.; Fujimoto, C.; Kim, Y. S. An operationally flexible fuel cell based on quaternary ammonium-biphosphate ion pairs. *Nature Energy* **2016**, *1* (9), 16120.

(16) Jackson, C.; Raymakers, L. F. J. M.; Mulder, M. J. J.; Kucernak, A. R. J. Assessing electrocatalyst hydrogen activity and CO tolerance: Comparison of performance obtained using the high mass transport floating electrode technique and in electrochemical hydrogen pumps. *Applied Catalysis, B: Environmental* **2020**, *268*, 118734. Jackson, C.; Raymakers, L. F. J. M.; Mulder, M. J. J.; Kucernak, A. R. J. Poison mitigation strategies for the use of impure hydrogen in electrochemical hydrogen pumps and fuel cells. *Journal of Power Sources* **2020**, *472*, 228476.

(17) Huang, F.; Pingitore, A. T.; Benicewicz, B. C. High polymer content m/p-polybenzimidazole copolymer membranes for electrochemical hydrogen separation under differential pressures. *Journal of Electrochemical Society*. **2020**, *167* (6), 063504.

(18) Huang, F.; Pingitore, A. T.; Benicewicz, B. C. Electrochemical Hydrogen Separation from Reformate Using High-Temperature Polybenzimidazole (PBI) Membranes: The Role of Chemistry. *ACS Sustainable Chem. Eng.* **2020**, *8* (16), 6234–6242.

(19) Lee, A. S.; Choe, Y.-K.; Matanovic, I.; Kim, Y. S. The energetics of phosphoric acid interactions reveals a new acid loss mechanism. *Journal of Materials Chemistry A* **2019**, *7* (16), 9867–9876.

(20) Venugopalan, G.; Chang, K.; Nijoka, J.; Livingston, S.; Geise, G. M.; Arges, C. G. Stable and Highly Conductive Polycation-Polybenzimidazole Membrane Blends for Intermediate Temperature Polymer Electrolyte Membrane Fuel Cells. *ACS Applied Energy Materials* **2020**, *3* (1), 573–585.

(21) Atanasov, V.; Lee, A. S.; Park, E. J.; Maurya, S.; Baca, E. D.; Fujimoto, C.; Hibbs, M.; Matanovic, I.; Kerres, J.; Kim, Y. S. Synergistically integrated phosphonated poly(pentafluorostyrene) for fuel cells. *Nature Materials* **2021**, *20* (3), 370–377.

(22) Lim, K. H.; Lee, A. S.; Atanasov, V.; Kerres, J.; Park, E. J.; Adhikari, S.; Maurya, S.; Manriquez, L. D.; Jung, J.; Fujimoto, C. Protonated phosphonic acid electrodes for high power heavy-duty vehicle fuel cells. *Nature Energy* **2022**, DOI: 10.1038/s41560-021-00971-x.

(23) Venugopalan, G.; Bhattacharya, D.; Kole, S.; Ysidron, C.; Angelopoulou, P. P.; Sakellariou, G.; Arges, C. G. Correlating high temperature thin film ionomer electrode binder properties to hydrogen pump polarization. *Materials Advances* **2021**, *2*, 4228–4234.

(24) Lee, K.-S.; Maurya, S.; Kim, Y. S.; Kreller, C. R.; Wilson, M. S.; Larsen, D.; Elangovan, S. E.; Mukundan, R. Intermediate temperature fuel cells via an ion-pair coordinated polymer electrolyte. *Energy Environmental Science* **2018**, *11* (4), 979–987.

(25) Nguyen, M. T.; Grigoriev, S. A.; Kalinnikov, A. A.; Filippov, A. A.; Millet, P.; Fateev, V. N. Characterisation of a electrochemical hydrogen pump using electrochemical impedance spectroscopy. *J. Appl. Electrochem.* **2011**, *41* (9), 1033.

(26) Thomassen, M.; Sheridan, E.; Kvello, J. Electrochemical hydrogen separation and compression using polybenzimidazole (PBI) fuel cell technology. *Journal of Natural Gas Science and Engineering* **2010**, *2* (5), 229–234.

(27) Wright, A. D.; White, V.; Hufton, J. R.; Quinn, R.; Cobden, P. D.; van Selow, E. R. CAESAR: Development of a SEWGS model for IGCC. *10th International Conference on Greenhouse Gas Control Technologies* **2011**, *4*, 1147–1154.

(28) Allam, R. J.; Chiang, R.; Hufton, J. R.; Middleton, P.; Weist, E. L.; White, V. Development of the Sorption Enhanced Water Gas Shift Process. In *Carbon Dioxide Capture for Storage in Deep Geologic Formations*, Vol. 1; Thomas, D. C., Benson, S. M., Eds.; Elsevier Science, 2005; pp 227–256.

(29) Wright, A.; White, V.; Hufton, J.; Selow, E. v.; Hinderink, P. Reduction in the cost of pre-combustion CO₂ capture through advancements in sorption-enhanced water-gas-shift. *Greenhouse Gas Control Technologies* **2009**, *1* (1), 707–714.

(30) Najmi, B.; Bolland, O.; Colombo, K. E. A systematic approach to the modeling and simulation of a Sorption Enhanced Water Gas Shift (SEWGS) process for CO₂ capture. *Separation and Purification Technology* **2016**, *157*, 80–92.

(31) Ribeiro, A. M.; Grande, C. A.; Lopes, F. V. S.; Loureiro, J. M.; Rodrigues, A. E. Four beds pressure swing adsorption for hydrogen purification: Case of humid feed and activated carbon beds. *AIChE Journal* **2009**, *55* (9), 2292–2302.

(32) Yang, S.-I.; Choi, D.-Y.; Jang, S.-C.; Kim, S.-H.; Choi, D.-K. Hydrogen separation by multi-bed pressure swing adsorption of synthesis gas. *Adsorption* **2008**, *14* (4), 583–590.

(33) Luberti, M.; Friedrich, D.; Brandani, S.; Ahn, H. Design of a H₂ PSA for cogeneration of ultrapure hydrogen and power at an advanced integrated gasification combined cycle with pre-combustion capture. *Adsorption* **2014**, *20* (2), 511–524.

(34) Zhu, X.; Shi, Y.; Li, S.; Cai, N. Two-train elevated-temperature pressure swing adsorption for high-purity hydrogen production. *Applied Energy* **2018**, *229*, 1061–1071.

(35) Matsumoto, H.; Okada, S.; Hashimoto, S.; Sasaki, K.; Yamamoto, R.; Enoki, M.; Ishihara, T. Hydrogen separation from syngas using high-temperature proton conductors. *Ionics* **2007**, *13* (2), 93–99.